JOURNAL OF GEOPHYSICAL RESEARCH: OCEANS, VOL. 118, 6854–6866, doi:10.1002/2013JC009367, 2013

On the dynamics of the seasonal variation in the South China Sea throughflow transport

Jiayan Yang,[1] Xiaopei Lin,[1,2] and Dexing Wu[2]

Received 22 August 2013; revised 12 November 2013; accepted 13 November 2013; published 16 December 2013.

[1] The Luzon Strait transport (LST) of water mass from the Pacific Ocean to the South China Sea (SCS) varies significantly with seasons. The mechanisms for this large variability are still not well understood. The steady-state island rule, which is derived from a steady-state model, is not applicable to seasonal time scale variations in a large basin like the Pacific Ocean. In this paper, we will use a theoretical model that is based on the circulation integral around the Philippines. The model relates the LST variability to changes in the boundary currents along the east coast of the Philippines, including the North Equatorial Current (NEC) Bifurcation Latitude (NECBL), the transports of Kuroshio and Mindanao Currents (KC and MC), and to the local wind-stress forcing. Our result shows that a northward shift of the NECBL, a weakening of the KC or a strengthening of the MC would enhance the LST into the SCS. This relationship between the LST and the NEC-KC-MC is consistent with observations. The analytical result is tested by a set of idealized numerical simulations.

Citation: Yang, J., X. Lin, and D. Wu (2013), On the dynamics of the seasonal variation in the South China Sea throughflow transport, *J. Geophys. Res. Oceans*, *118*, 6854–6866, doi:10.1002/2013JC009367.

1. Introduction

[2] The South China Sea (SCS) is a large semienclosed marginal sea with several straits that are connected to the Pacific and Indian Oceans. The Luzon Strait is the deepest passage (>2000 m in depth) through which there is a net westward transport from the Pacific Ocean into the SCS [*Wyrtki*, 1961; *Qu et al*., 2000; *Yaremchuk and Qu*, 2004; *Tian et al*., 2006]. The transport into the SCS through the Luzon Strait is balanced by outflows to the East China Sea (ECS) through the Taiwan Strait (<200 m in depth), to the Sulu Sea through the Mindoro Strait (<200 m in depth) and to the Java Sea via the Karimata Strait (<100 m in depth). This interbasin flow system, as schematized in Figure 1a, forms a South China Sea Throughflow (SCSTF) and serves as an important route for Indo-Pacific exchanges [*Qu et al*., 2005; *Yu et al*., 2007; *Yaremchuk et al*., 2009]. Many previous studies showed that the intrusion of the Kuroshio water into the SCS is highly seasonal [*Centurioni et al*., 2004]. Several mechanisms likely contribute to this seasonality, including local wind stress and its curl on both sides of Luzon Strait [e.g., *Farris and Wimbush*, 1996; *Metzger and Hurlburt*, 2001; *Jia and Chassignet*, 2011; *Wu and Hsin*, 2012]. In a recent study, *Wu and Hsin* [2012] argued that the northeasterly wind in winter forces a westward Ekman transport and contributes to a larger transport in winter. It was not clear whether the Ekman transport would enhance the net transport through the Strait. As we will show later in Figure 6, an intrusion of the Kuroshio water is not necessarily the same as the net SCSTF transport—the integrated transport across the strait.

[3] The Luzon Strait Transport (LST), which has been commonly used to measure the SCSTF, varies considerably with the seasons. It increases from as low as near 0 Sv in the summer to as high as 5 Sv in the late fall and the early winter according to *Yaremchuk and Qu* [2004]. This large seasonal variability was also revealed by trajectories of satellite-tracked drifters [*Centurioni et al*., 2004] and mooring acoustic Doppler current profilers [*Liang et al*., 2008]. The dynamical underpinning for this seasonal variability remains not well understood. Previous studies [e.g., *Yaremchuk and Qu*, 2004] indicated some coherences between seasonal variations in the LST and in boundary currents along the east coast of the Philippines. The goal of this study is to examine their dynamical linkage and to develop a better understanding of the leading mechanism for the seasonal variability of the LST.

[4] The SCSTF is primarily wind driven and so the island rule [*Godfrey*, 1989] has been used to examine both the mean transport and its interannual variability [*Qu et al*., 2000; *Wang et al*., 2006a, 2006b]. The original island rule is based on the steady Sverdrup dynamics in the open ocean. So it applies only to variations with periods that are considerably longer than the adjustment time scale of the wind-driven circulation in the vast open ocean to the east of the island. A baroclinic Rossby wave would take longer

[1]Department of Physical Oceanography, Woods Hole Oceanographic Institution, Woods Hole, Massachusetts, USA.
[2]Physical Oceanography Laboratory, Ocean University of China, Qingdao, China.

Corresponding author: J. Yang, Department of Physical Oceanography, Woods Hole Oceanographic Institution, Woods Hole, MA 02543, USA. (jyang@whoi.edu)

2169-9275/13/10.1002/2013JC009367

than 1 year to propagate across the Pacific basin from the Central American coast to the east coast of the Philippines. Oceanic currents along the western boundary, including the LST, cannot be in equilibrium state with wind-stress forcing over the Pacific Ocean on the seasonal time scale [*Qiu and Lukas*, 1996] and so the island rule is not suitable for studying the seasonal variability of the LST. *Firing et al*. [1999] extended the island rule to time-dependent flows. A main difference is the addition of a storage term that relates to the thermocline depth changes in the area to the east of the island. Additional information is needed to compute this time-dependent storage term. Furthermore, there is an uncertainty regarding whether the island rule, even in the time-dependent form, is applicable to the SCS where there are multiple passages, and therefore possibly multiple choices for integration contours in the island rule. Here we will derive a relationship that is based mainly on the momentum balance along the east coast of the Philippines between point A and point C in Figure 1a.

[5] The atmospheric circulation in the region is highly seasonal and closely tied to the Asian Monsoon (Figure 2). The surface wind is predominantly northeasterly in the winter and reverses to southwesterly in the summer. The LTS variability is closely tied to variations in three major currents off the east coast of the Philippines, namely the Kuroshio and Mindanao Currents (KC and MC) along the coast and the North Equatorial Current (NEC)—a westward interior current that eventually impinges on the coast of the Philippines (Figure 1a). The NEC, once it reaches the east coast of the Philippines, bifurcates to form the KC and MC—two western boundary currents (WBC) that flow in opposite directions. The NEC bifurcation latitude (NECBL) varies seasonally between 13° and 15°N off the coast of the Philippines according to observations and model simulations. A descriptive relationship has been established between the LST variability and variations in the NEC-KC-MC [*Yaremchuk and Qu*, 2004]. In this paper, we seek to develop a simple model that can explain the essential dynamics in this linkage.

[6] The remainder of the paper is organized as follows. In section 2, we will review previous studies of seasonal variations in the NEC-KC-MC along the east coast of the Philippines, the LST variability, and the local wind-stress forcing. In section 3, we will compare results from a numerical simulation that uses a realistic wind stress and geometry with the island rule. In section 4, we will formulate a simple analytical model that links the LST to boundary currents and wind stress. Results from several idealized simulations will be used to test the analytical solution. Some further discussion and a brief summary will be given in section 5.

2. The LST and the Low-Latitude WBCs in the North Pacific Ocean

[7] Direct measurements of the LST are scarce. So LST variability has been mainly estimated from geostrophic calculations from hydrographic data and/or from the sea surface height (SSH) measured by satellite altimeters. Numerical simulations, especially those with data-assimilation, add additional insights. The LST, according to previous studies, varies strongly with the seasons,

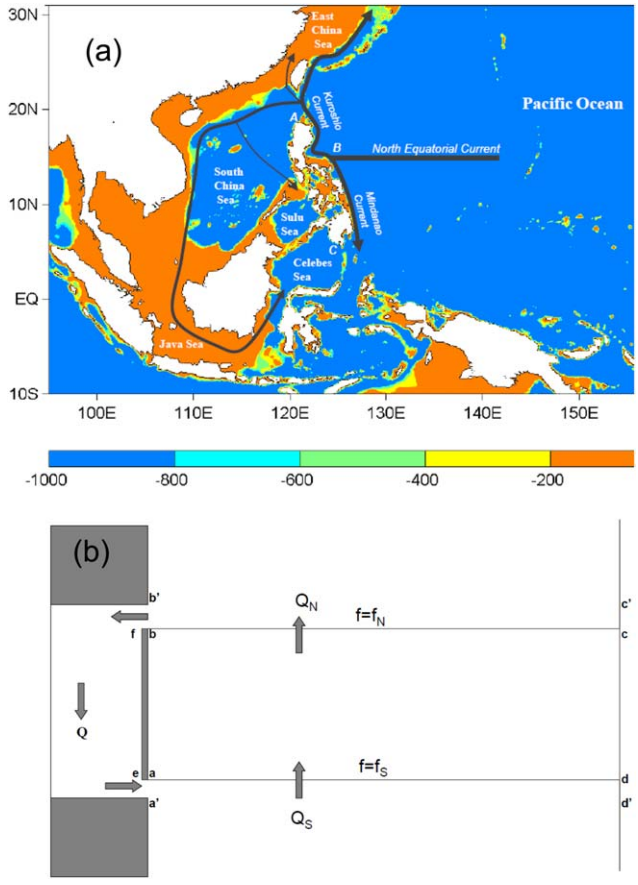

Figure 1. The bathymetry in the vicinity of the SCS (color in the top plot) with schematics of major currents in the region. The SCS Throughflow pathways are from *Qu et al*. [2005]. (bottom) Schematic of the island rule integration. In the classic island rule [*Godfrey*, 1989], the transport around the island depends solely on the wind stress along the close line $l = cfedc$ and the planetary vorticity difference between the two extremities of the island, $\Delta f = f_N - f_S$.

strengthening in the fall and early winter and weakening in the summer. In a comprehensive analysis of both the sea surface height (altimetry) and hydrographic data, *Yaremchuk and Qu* [2004] showed that the geostrophic transport through the Luzon Strait varies from as low as 0–1 Sv in August to as high as 5 Sv in December. This pattern of seasonal changes is consistent with trajectories of satellite-tracked drifts reported by *Centurioni et al*. [2004].

[8] Along the east coast of the Philippines, the flow is strongly dominated by several major currents that include the NEC, KC, and MC. The latter two are formed when the NEC impinges on the east coast of the Philippines and bifurcates to two boundary currents, i.e., the northward KC, and the southward MC [*Nitani*, 1972]. This low-latitude NEC-KC-MC current system varies considerably on both seasonal and interannual time scales [*Toole et al*., 1988, 1990; *Qiu and Lukas*, 1996; *Qu and Lukas*, 2003; *Qiu and Chen*, 2010]. It has been postulated that the seasonal variability of the LST is influenced by variations in the NEC bifurcation latitude (NECBL) and transports of KC and MC [*Yaremchuk and Qu*, 2004]. In situ observations

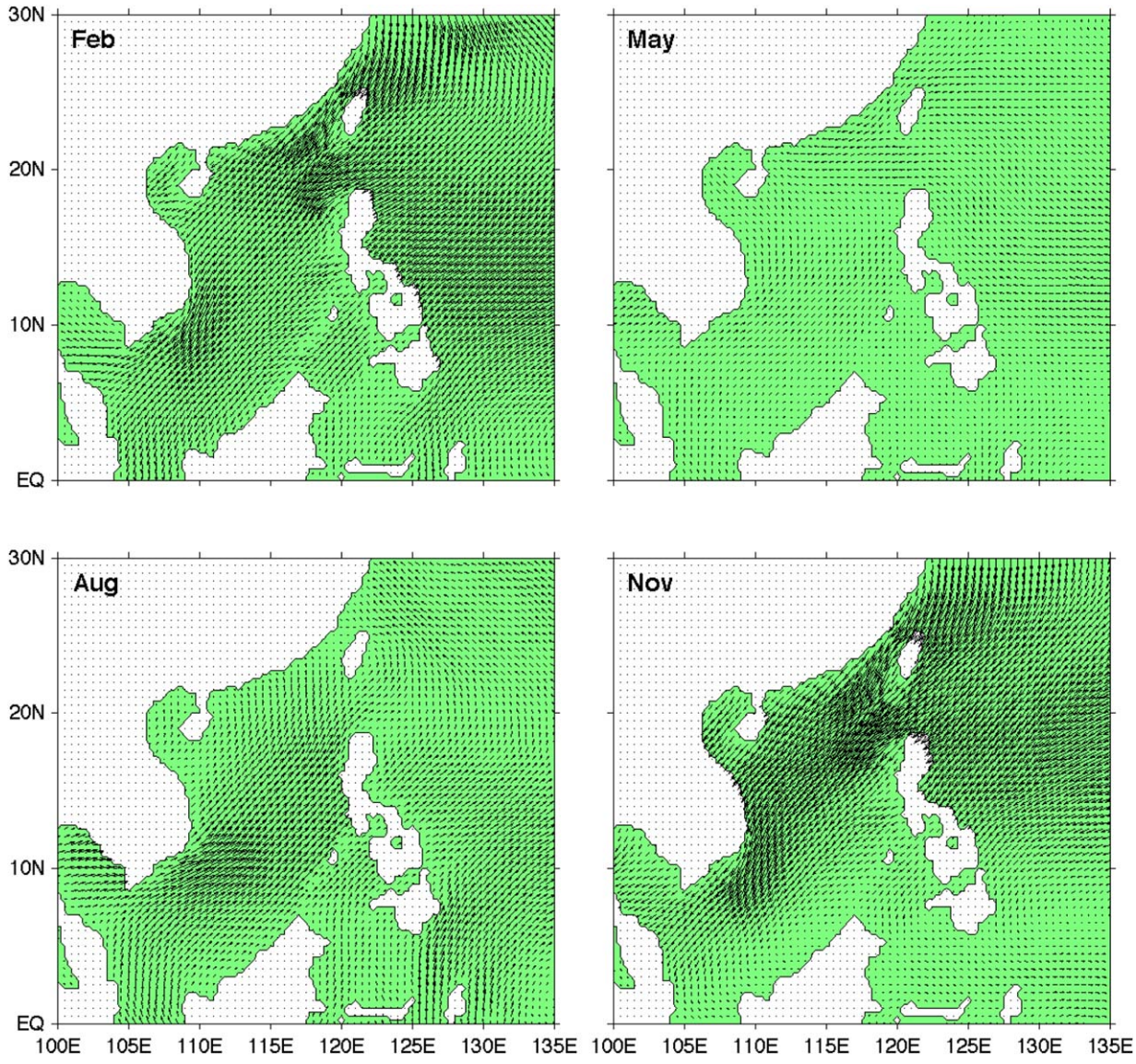

Figure 2. Surface wind stress in the vicinity of the South China Sea (the wind stress is from the monthly mean climatology product from the Objective Analyzed Flux Wind, OAFlux-Wind (L. Yu, http//:oaflux.whoi.edu). It is derived from a 21 year daily product from 1988 to 2008, an era with satellite wind stress observations. The surface wind is monsoonal and reverses its direction seasonally.

indicate that the NECBL is located at about 13N [*Toole et al*., 1988, 1990]. But *Qu and Lukas* [2003] argued that the NECBL moves northward with depth and so the depth-averaged position should be located north of 13N. *Yaremchuk and Qu* [2004] combined altimetry and hydrography data and showed that the NECBL moves southward to 13.8N in the summer and northward to 15.8N in the fall. They estimated that the mean position of NECBL is at 14.3N. This pattern of the seasonal movement was consistent with what was found earlier by *Qu and Lukas* [2003] who suggested that the NECBL is located in the southernmost latitude in July and the northernmost latitude in December.

[9] In addition to the seasonal excursion of the NECBL, both the KC and MC vary considerably in their transports. The KC is weak in the fall while the MC transport is seasonally low in the summer. The annual mean transports are 27.6 and 30.1 Sv, respectively, for KC and MC off the Philippines coast [*Yaremchuk and Qu*, 2004]. The main seasonal variability of low-latitude WBCs along the Philippines coast is summarized as follows. The NECBL shifts northward and KC weakens in the fall. The NECBL moves southward and MC transport decreases in the summer. But we will like to point out that the KC and MC vary on seasonal and interannual time scales. There are considerable differences in previous estimates.

3. The Island Rule and Seasonal Variation in the LST

[10] The spin-up time scale of a wind-driven gyre in a large basin like the Pacific Ocean is typically longer than 1 year. The premise of this study is that the island rule, which is derived from a steady state model, does not apply to the

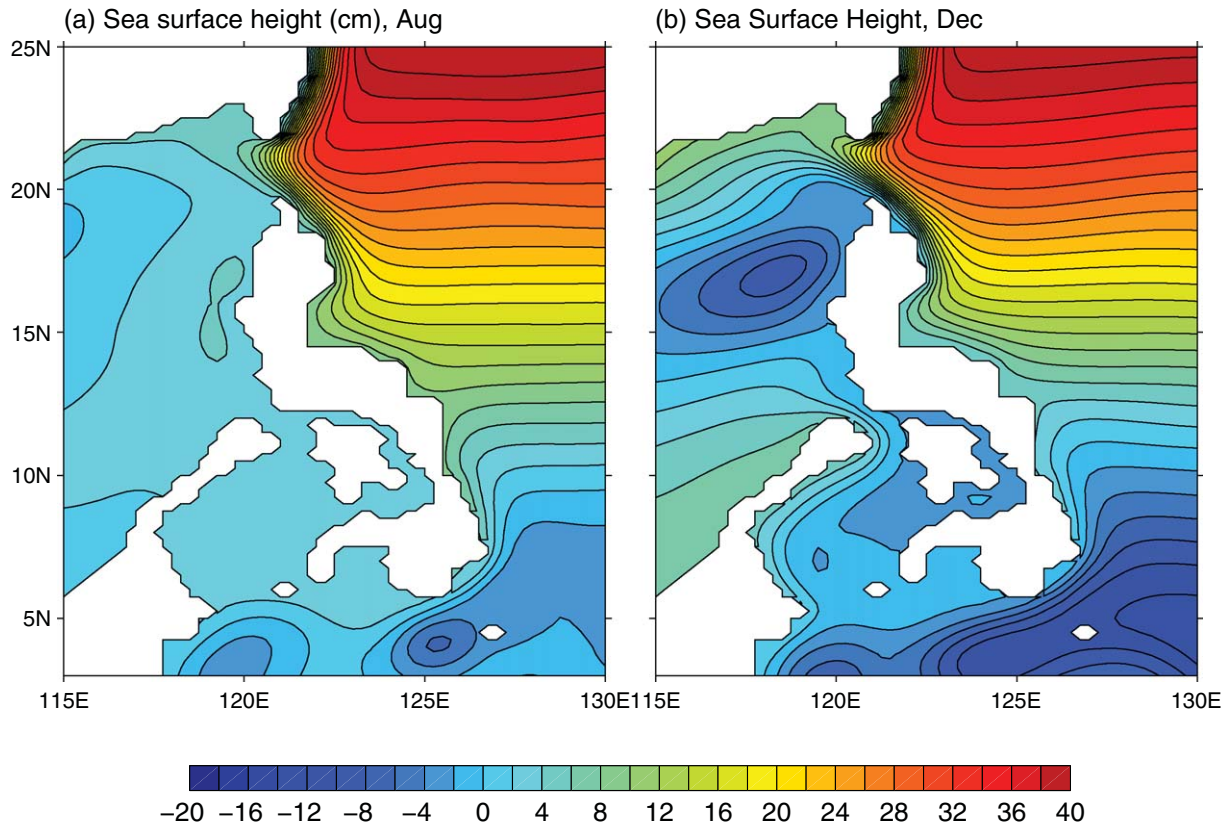

Figure 3. The sea surface height (SSH, unit: cm), in August and December, produced by a nonlinear and reduced-gravity model forced by the OAFlux-Wind (Figure 2). The transport is maximum in December and minimum in August, and is consistent with an observation-based estimate. The seasonal movement of the phase of the NECBL movement is consistent with the observation that it moves to the northernmost position in fall and the southernmost latitude in summer. The extent of the seasonal movement of the NECBL is smaller than the observation, a model feature that was noted and explained by *Qiu and Lukas* [1996].

seasonal variability of the LST. Here we will test this assumption by using a one-layer nonlinear and reduced-gravity model. The model is governed by the following equation:

$$\frac{d\vec{u}}{dt}+f\vec{k}\times\vec{u}=-g'\nabla h+\frac{\vec{\tau}}{\rho h}+A_H\nabla^2\vec{u}$$
$$\frac{\partial h}{\partial t}+\nabla\cdot(h\vec{u})=0 \qquad (1)$$

where $h=h_0+h'$ is the layer thickness ($h_0=400$ m), $g'=0.0156$ ms^{-2} is the reduced gravity and its value is chosen so that the shallow-water gravity wave speed $C=(g'h_0)^{1/2}=2.5$ ms^{-1} represents the first baroclinic mode. The model uses lateral mixing for the momentum dissipation with a viscosity $A_H=1000$ m^2 s^{-1}. A large viscosity is used so that the frictional Munk boundary layer can be better resolved in the model [*Yang*, 2003]. The model uses a staggered C-grid. Two sets of experiments will be used, one with a realistic coastline and observation-based wind stress and the other with idealized forcing and model geometry. The idealized experiments will be introduced and discussed in section 4 after the analytical model is presented. In this section, we will discuss the results from a simulation forced by a realistic wind stress.

[11] The model extends from 20S to 45N with a resolution of 1/4°. We use the wind stress from the monthly climatology from the Objectively Analyzed Flux-Wind (OAFlux-Wind) (L. Yu, http//:oaflux.whoi.edu). It is a climatology that was derived from a 21 year daily product from 1988 to 2008, an era with satellite wind stress observations. Figure 2 shows the OAFlux wind stress in February, May, August, and November. The northern and southern boundaries are closed.

[12] This simple reduced-gravity model, like other similar ones in previous studies, is capable of simulating some basic features of basin-wide circulations, including the subtropical gyre and equatorial currents that are relevant to the LST. Here we will only discuss the transport through the Luzon Strait and flows around the Philippines. Figure 3 shows the sea surface height (SSH) in August and December—when the minimum and maximum LST transports occur as reported by *Yaremchuk and Qu* [2004]. The monthly averaged transport is <0.1 Sv in August and reaches 7.4 Sv in December. The seasonal variability of the LST transport is shown in Figure 4a. The overall pattern of the seasonal variation in the LST is very similar to that derived from data [*Yaremchuk and Qu*, 2004, Figure 14 in their paper] except that the amplitude is considerably larger

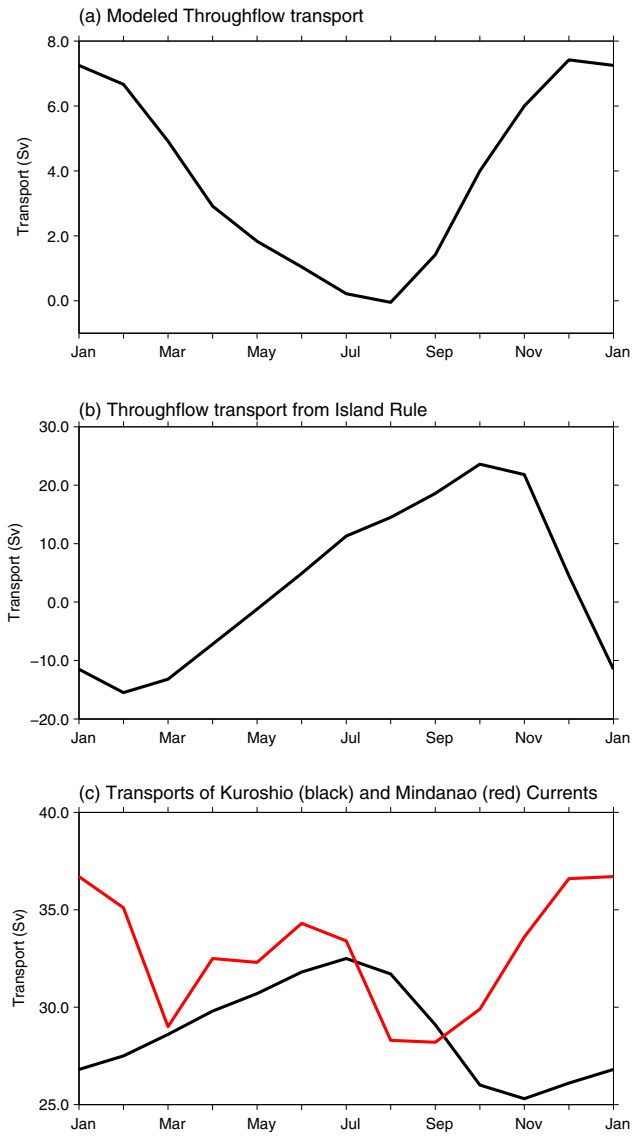

Figure 4. (top) Seasonal variation of the monthly mean LST (positive for the westward transport into the SCS in the northern strait). The variation is similar to the observation-based estimation [*Yaremchuk and Qu*, 2004; *Yaremchuk et al*., 2009]. (middle) The seasonal transport computed from the Island Rule [*Godfrey*, 1989]. It shows that the island rule does not apply to the LST on the seasonal time scale. The lower panel shows the transports of Kuroshio (black line) and Mindanao Current (red line). When the LST is strong in the fall, the Kuroshio is weak and the Mindanao is strong, and vice versa in the summer.

in the model. *Yaremchuk and Qu* [2004] showed that LST varies from 0–1 Sv in August to about 5 Sv in December. But a more recent update from *Yaremchuk et al*. [2009] revised the seasonal variation that ranges from 1 Sv in July to about 7 Sv in January. So the magnitude of the model transport compares more favorably with the latter.

[13] Is the island rule able to capture this seasonal variability in the LST? Following *Godfrey* [1989], we integrate the linear version of the momentum equation (1) along a closed path $l = fedcf$, a thin black line shown in Figure 1b:

$$\frac{\partial}{\partial t}\oint_l h\,\vec{u}\cdot d\vec{l} + (Q_N f_N - Q_S f_S) = \oint_l \vec{\tau}_{wind}\cdot d\vec{l} \tag{2}$$

[14] In a steady state, there is no convergence of mass flux into the area bounded by l and so $Q_N = Q_S$ in (2). The time change of the circulation integral, the first term in (2), is also zero in a steady state. So equation (2), in a steady state, becomes:

$$Q_{island-rule} = \frac{1}{\Delta f}\oint_l \vec{\tau}_{wind}\cdot d\vec{l} \tag{3}$$

where $Q_{island\text{-}rule} = Q_N = Q_S$ in a steady state and $\Delta f = f_N - f_S$. This is the original form of Godfrey's island rule. When applied to the SCSTF, the integration is along a closed path l along the west coast of the Philippines, across the Pacific Ocean from the southern tip of the island, c in Figure 1a, to the eastern oceanic boundary, continuing along the eastern boundary to the latitude of the northern tip of the island (a in Figure 1a, which is also the southern boundary of the Luzon Strait), and zonally across the Pacific Ocean to the northern coast of the Philippines, and $\Delta f = f_N - f_S$ is the difference of the planetary vorticity f between a and c in Figure 1a.

[15] Figure 4b shows the seasonal variability of the LST transport that is derived by the island rule (3) by using the same OAFlux wind stress as that applied in the numerical model shown in Figures 3 and 4a. It varies from −15 Sv in February to 22 Sv in October. Both the phase and the amplitude are very different from the model result (Figure 4a) and also different from any observation-based estimates from previous studies [e.g., *Yaremchuk and Qu*, 2004]. Obviously the island rule does not apply to the LST on the seasonal time scale.

[16] What can cause such a large difference between the numerical simulated result (Figure 4a) and the island rule estimate (Figure 4c)? Is it the nonlinearity that was neglected by *Godfrey* [1989]? Our analysis indicates that the nonlinear effect is small and not responsible for the difference between Figures 4a and 4b. Another possibility is the friction along the oceanic eastern boundary and the northern, southern, and western coasts of the Philippines. Friction along these segments is ignored in the island rule. As discussed in previous studies [e.g., *Pedlosky et al*., 1997; *Pratt and Pedlosky*, 1998; *Wajsowicz*, 1993], the friction only plays a small role unless the west coast of the island is close to the oceanic western boundary (in our application, it would be the Vietnamese and Chinese coasts) according to *Pratt and Pedlosky* [1998]. Furthermore, the friction tends to reduce the transport not to change the phase of the temporal variations. So it is very unlikely that the friction has played any role in the difference between the model and IR. Topographic effect or the bottom pressure torque is also neglected in IR. It may weaken transport substantially between the open ocean and the marginal sea. But in our recent analysis [*Yang et al*., 2013], the topographic barrier weakens near the equator. This may help explain why the island rule is able to give a reasonable estimate of the SCS throughflow transport in the mean state despite that it exits the SCS through shallow straits.

[17] Figure 4c shows the seasonal variations of the KC and MC transports, indicating the transient forcing from the

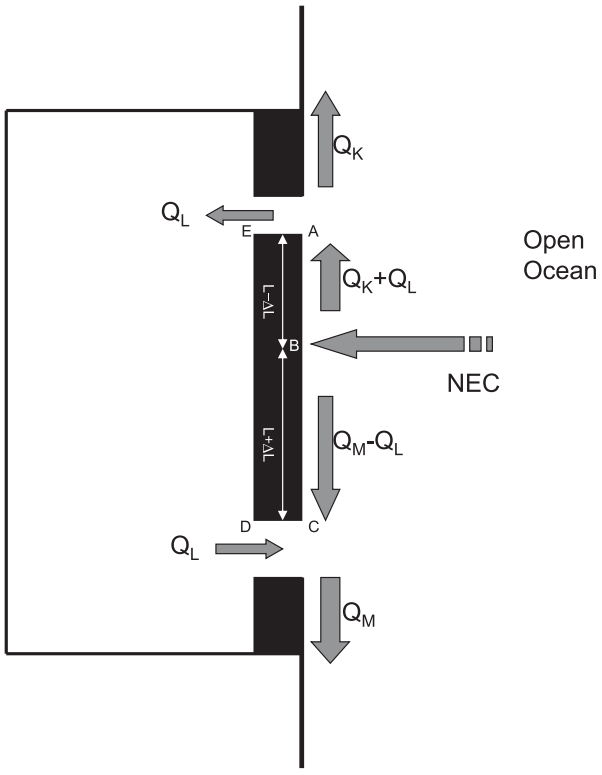

Figure 5. The schematic of our analytical model.

ocean interior. One could use the time-dependent form of the island rule, i.e., equation (2), for the seasonal variability of the LST. A similar form has been used by *Firing et al.* [1999] in their study of the Hawaiian Ridge Currents. But the most attractive feature in the island rule is its mathematical simplicity and its dynamical transparency. The transport into the area bounded by l is no longer nondivergent since the thermocline depth variation changes the upper-layer water volume within the area bounded by l. An additional model is needed for computing the thermocline depth changes.

4. The Seasonal Variability in the LST and Its Relationship to the NEC-KC-MC and the Local Wind Stress

[18] We have argued that the island rule, in either a steady or a time-dependent form, is not ideal for studying the dynamics that control the seasonal variability in the LST. A simple dynamical framework is still needed. Here we will try to formulate a dynamical relationship between the LST and the NEC-KC-MC. Observation-based analyses show that the NEC bifurcation and the partition of KC and MC transports vary seasonally. The bifurcation is displaced northward and the KC is weaker in the fall when the LST is strongest, and vice versa in the summer when the LST is weak. We will derive an analytical relationship based on a reduced-gravity model with Munk WBC layer dynamics. This will be followed by a set of idealized experiments to test the analytical solution.

[19] Consider an idealized model that is schematized in Figure 5. An idealized SCS is separated from the open ocean by an island, with a coast line $l = ABCDE$, that is meant to represent several islands of the Philippines. Two straits connect the SCS to the open ocean. The northern channel is for the Luzon Strait and all southern SCS passages are collectively represented by one southern channel. A westward North Equatorial Current bifurcates at point B and forms a northward Kuroshio and a southward Mindanao Current. Transient adjustment for the pressure around the island involves fast Kelvin waves. The 1st baroclinic mode Kelvin waves typically travel at a speed of 2–3 m/s and would take less than a month to propagate around an island that has the size of the Philippines. Follow *Pratt and Pedlosky* [1998] we can rewrite equation (1) as

$$\frac{\partial \vec{u}}{\partial t} + (f+\xi)\vec{k}\times\vec{u} = -\nabla\left(\frac{\vec{u}\cdot\vec{u}}{2} + g'h\right) + \frac{\vec{\tau}_{wind}}{h} + \vec{F} \tag{4}$$

where $h = h_0 + h'$ is the layer thickness and $\vec{F}$ is the friction. Now let's integrate equation (4) around the island's coast $l = ABCDEA$. Along a solid boundary the first term is zero due to the no-slip boundary condition and the second term is also zero due to the no-normal flow condition. The integral of the first term on the right hand side around a closed path around the island ($l = ABCDEA$) is zero. So the integral of equation (4) is simplified to:

$$\oint_{l=ABCDEA}\left(\frac{\vec{\tau}_{wind}}{h} + \vec{F}\right)\cdot d\vec{l} = 0 \tag{5}$$

[20] It is worth noting that we do not assume the flow is steady in this model. The change of the circulation around the island is zero due to the nonslip boundary condition. So the friction and the wind stress have to adjust to each other instantaneously.

[21] Following the same argument made by *Godfrey* [1989] and *Pedlosky et al.* [1997], we assume that the friction is important only along the island's east coast ABC where a frictional western boundary layer exists, i.e., $\oint_{l=ABCDEA}\vec{F}\cdot d\vec{l} \approx \int_{y=y}^{y=y_C} F dy$. equation (5) becomes:

$$\oint_{l=ABCDEA}\left(\frac{\vec{\tau}_{wind}}{h}\right)\cdot d\vec{l} + \int_{y=y}^{y=y_C} F dy = 0 \tag{6}$$

4.1. The Roles of the NEC, KC, and MC

[22] First, we would like to separate the local wind stress effect from the WBC dynamics. Here we assume that the local wind stress is negligible, and equation (6) becomes

$$\int_{y=y}^{y=y_C} F dy = 0 \tag{7}$$

[23] Equation (7) indicates that the friction induced by the western boundary current cannot be unidirectional along the island's east coast ABC. If the model uses the Stommel WBL, the friction has the form, $\vec{F} = -\lambda\vec{u}$ (λ is a linear drag coefficient) and (7) becomes:

$$-\lambda\int_{y=y}^{y=y_C} v\, dy = 0 \tag{8a}$$

[24] If the model uses the Munk WBL model, (which was used in our numerical model (1)), equation (7) becomes:

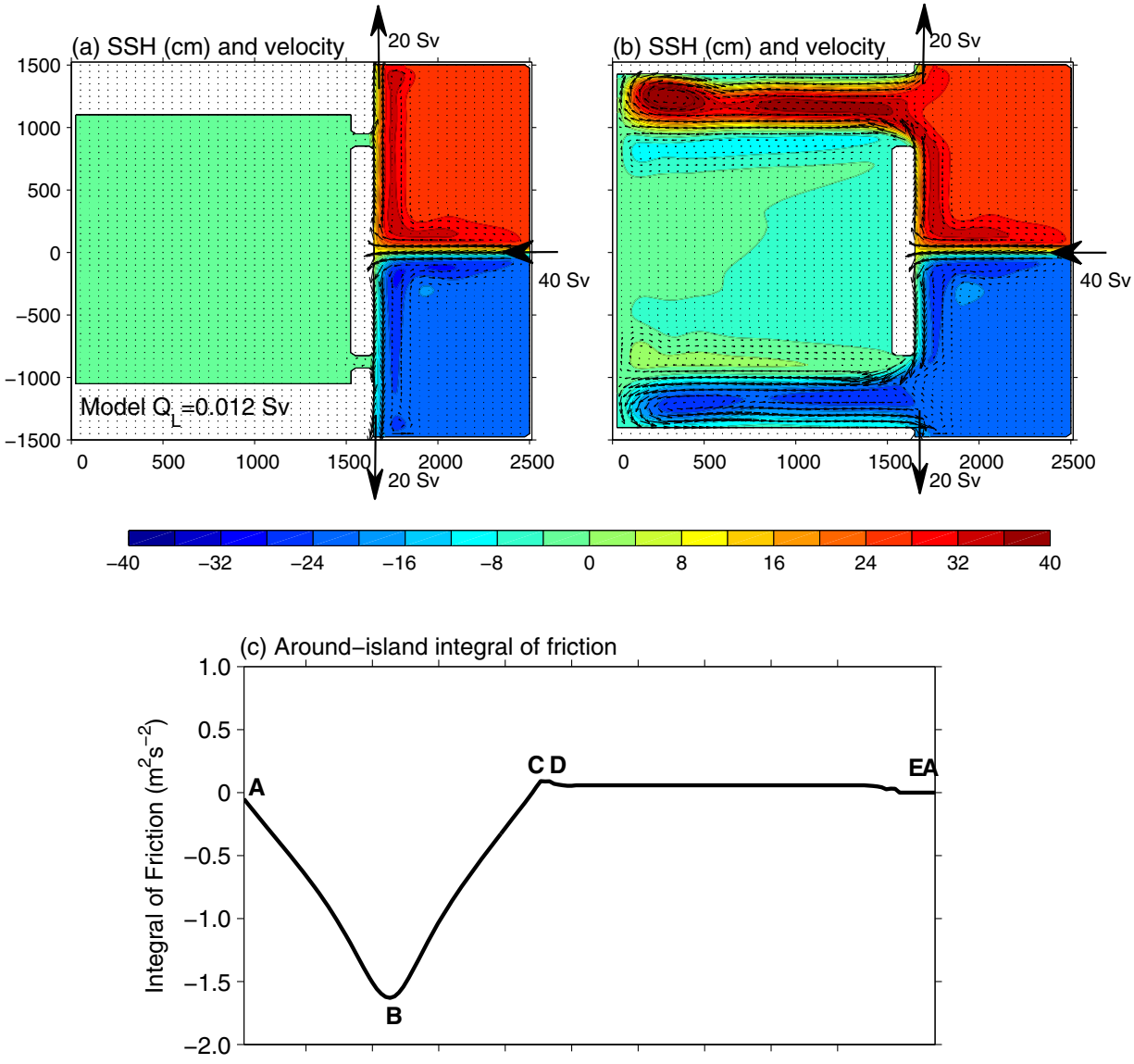

Figure 6. (a) The SSH and velocity in the first idealized experiment using a nonlinear and reduced-gravity model. The model is forced by prescribed inflow and outflows. In this experiment, the forcing is symmetric, i.e., a westward inflowing NEC is located at $y = 0$, and two outflows with equal transport are specified on the northern and southern boundary, respectively. The throughflow transport is negligible (0.012 Sv); (b) a similar experiment but with widened gaps. *Sheremet* [2001] showed that whether a WBC can leap over a gap depends on a ratio between the width of the gap and the Munk WBL width. This experiment shows that our result remains valid even if the WBCs cannot leap over the gaps and have to make detours within the marginal sea The net throughflow transport remains very small in this case (<0.1 Sv); (c) a clockwise integration of the friction along the island's boundary. It shows that the accumulative friction exerted by the northward WBC (from A to B) cancels that induced by the southward boundary current (B to C). The friction along the west coast (D to E) is negligible. Through this integral constraint, we can formulate a simple model that relates the throughflow transport to the strengths and lengths of the WBCs along the island's east coast.

$$\int_{y=y}^{y=y_C} A_H \partial^2 v/\partial x^2 dy = 0 \tag{8b}$$

[25] Note: The assumption that $|\partial^2 v/\partial y^2| \ll |\partial^2 v/\partial x^2|$ is invalid within a narrow width of the NEC incidence at the wall. Within this width, v increases rapidly in the y direction. The overall scaling argument that the integrated friction is proportional to the WBC transport remains valid.

[26] Either (8a) or (8b) requires that the velocity along the east coast of the island cannot be unidirectional. So the incoming NEC must bifurcate to two boundary currents with opposite directions, i.e., the Kuroshio and Mindanao Currents. The velocity integral from the southern to the northern tip of the island must be zero. To be consistent with our numerical model, we will use the Munk WBL model in the following analyses. The result will remain

qualitatively the same if we use the Stommel model. Equation (8b) can be written as:

$$\int_{y=y}^{y=y_B} A_H \partial^2 v/\partial x^2 dy + \int_{y=y}^{y=y_B} A_H \partial^2 v/\partial x^2 dy = 0 \qquad (9)$$

[27] The essence of equation (9) is that the total accumulated friction exerted by the Kuroshio along the island's coast must exactly cancel that induced by the Mindanao Current. Equation (9) is derived from integration of the momentum equation around the island in a time-dependent, nonlinear and one-layer model. The basic dynamics can be better illuminated in terms of linear dynamics of boundary currents. In absence of a local wind-stress forcing, the zero-order dynamical balance along a boundary is:

$$\left(-\frac{1}{\rho}\nabla p + \vec{F}\right)\cdot\vec{l} = 0 \qquad (10)$$

[28] As noted earlier, both the inertia and Coriolis force terms vanish along a boundary due to the nonslip and no-normal flow boundary conditions. The pressure gradient along the island's west coast is zero due to the lack of a frictional boundary layer (any initial pressure gradient would be erased by Rossby-wave radiation). So the pressure must be the same between point *E* and point *D* in Figure 5. One could make a similar argument regarding a northern or southern boundary layer and assume that the pressure is the same between *A* and *E*, and between *D* and *C*. These are the same assumptions that were made in previous studies of flows around an island [*Pedlosky et al*., 1997; *Pratt and Pedlosky*, 1998]. With these assumptions, the pressure at *A* must be the same as that at *C*, i.e., $p_A = p_C$. Integrating (10) from *A* to *C* yields:

$$\int_{y=y_A}^{y=y_C} F dy = \frac{1}{\rho}(p_C - p_A) = 0$$

[29] This is the same as equation (7). So the integrated friction from the southeastern tip of the island *C* to the northeastern corner *A* must be zero. In other words, the integrated friction induced by the Kuroshio Current along the island's east coast must cancel exactly that inflicted by the Mindanao Current.

[30] In the Munk (or Stommel) WBL model, the friction is therefore proportional to the magnitude or the transport of the boundary current, i.e., $\int_{y=y}^{y=y_2} A_H \partial^2 v/\partial x^2 \mathrm{d}y \propto Q(y_2 - y_1)$ (where Q is the WBC transport). The WBC transport Q off the coast of the Philippines between the NECBL and the Luzon Strait consists of two parts, the Kuroshio Current transport due to the subtropical gyre in the Pacific Ocean Q_K and the SCSTF transport through the Luzon Strait Q_L, i.e., $Q = Q_K + Q_L$. Similarly, the WBC transport south of the NECBL can be decomposed to $Q = Q_M - Q_L$, where Q_M is the WBC transport associated with the North Pacific tropical gyre. With these notations, equation (9) becomes:

$$(y_A - y_B)(Q_K + Q_L) = (y_B - y_C)(Q_M - Q_L) \qquad (11)$$

[31] Let's assume the total meridional length of the island is *2L* and the NECBL is a distance of ΔL northward of the central position of the island (or southward of the central position if ΔL is negative) as depicted in Figure 5. So (11) can be expressed as:

$$(L - \Delta L)(Q_K + Q_L) = (L + \Delta L)(Q_M - Q_L)$$

[32] A rearrangement gives a simple relationship between the transport through the Luzon Strait (Q_L), the NECBL (ΔL) and transports of the Kuroshio and Mindanao Currents (Q_K and Q_M):

$$Q_L = (Q_M - Q_K)/2 + \Delta L(Q_M + Q_K)/2L \qquad (12)$$

[33] Equation (12) is derived from a circulation integral constraint around an island. The same result is implicit in previous studies of the island rule [e.g., *Pedlosky et al*., 1997; *Pratt and Pedlosky*, 1998; *Firing et al*., 1999]. Here we emphasize the application of equation (12) in explaining the relationship between LST and the Kuroshio and Mindanao Currents, rather than the theoretical novelty of equation (12).

[34] What does equation (12) mean in terms of dynamics? First let's consider a special case in which the NECBL is located right at the center position of the island, i.e., $\Delta L = 0$. The LST, which becomes $Q_L = (Q_M - Q_K)/2$ according to (12), would increase when the Mindanao Current strengthens or when the Kuroshio Current transport weakens, and vice versa. This seems counter intuitive considering that the LST is supplied by the Kuroshio Current. One would expect intuitively that a stronger Kuroshio would lead to a greater transport into the SCS. Our solution, $Q_L = (Q_M - Q_K)/2$, is actually consistent with previous observation-based studies. The LST Q_L peaks in October–December when the Kuroshio transport is at its seasonally minimum while Q_L is weak in May–September when the Kuroshio Current is strongest [*Yaremchuk and Qu*, 2004]. How do we make sense of this relationship?

[35] The dynamics behind this relationship can be explained in terms of the dynamical constraint expressed by (9) or (11). When the two WBCs, i.e., the KC and MC, have the same lengths along the east coast of the island (i.e., $y_A - y_B = y_B - y_C$), the WBC transports north and south of the NECBL must have the same magnitude so that the friction exerted by them can cancel each other when integrated from A to C in Figure 5, i.e., $Q_K + Q_L = Q_M - Q_L$. When the northward KC transport (Q_K) weakens, the LST (Q_L) must increase to enhance the net northward WBC transport ($Q_K + Q_L$) and to weaken the net southward WBC transport ($Q_M - Q_L$) so that the two transports have the same magnitude, and vice versa when the Kuroshio strengthens.

[36] Now let's consider another special case in which the transports of the Kuroshio and Mindanao Currents are equal (i.e., $Q_K = Q_M$) but the NECBL is shifted away from the center position of the island. The LST, according to equation (12), becomes $Q_L = \Delta L Q_K / L$. The transport Q_L is positive (into the SCS via the northern strait) when the NECBL moves northward (i.e., $\Delta L > 0$) and negative when the NECBL shifts southward. The dynamics can be explained as follows. When the NECBL shifts northward, the northward WBC runs a shorter length before reaching

the northeastern corner of the island. Therefore, the northward WBC transport must be enhanced so that the total integrated friction over this shorter path can counter the friction exerted by the southward WBC that runs over a longer distance. An increased LST Q_L can fulfill this requirement.

[37] Next, we will examine the analytical solution (12) by using results from some idealized experiments. The same one-layer model, described by (1), is used. Most parameters remain the same as that used in the more realistic simulation shown in Figure 3. All boundaries are closed except where the inflow and outflow are prescribed. No-normal flow and no-slip conditions are applied along the solid boundary. The model is coded on a β-plane that is centered at 20N in latitude. Its domain extends 3000 km meridionally and 2500 km zonally. The model resolution is 25 km and uses an Arakawa C grid. In each experiment, the model was run 40 years and the model reaches a steady state.

4.1.1. Model Response to the NECBL Movement

[38] In the first set of experiments, an westward zonal jet is prescribed at the center of the eastern boundary to represent the NEC (this zonal jet will be hereafter referred as "NEC" even though it is prescribed as a boundary condition instead of being formed by the convergence of the Sverdrup transport in the real ocean). The NEC bifurcates to two boundary currents once it reaches the east coast of a meridionally elongated island. A semienclosed marginal sea is separated from the open ocean by this island. The NEC transport is prescribed to be 40 Sv and the mass balance is achieved by prescribing two outflowing western boundary currents, representing a northward Kuroshio and a southward Mindanao Current, along the northern and southern boundaries. The sum of these two WBCs is 40 Sv but their partition varies in each experiment.

[39] In the first experiment, the forcing is symmetrical with an inflow NEC specified right at the central position between $y = -50$ and 50 km on the eastern boundary. The outflow is split evenly to 20 Sv along both northern and southern boundary. The throughflow transport, according to our analytical solution (12), should be zero. The model indeed produces a negligible throughflow transport of 0.012 Sv. Figure 6a shows the SSH and the velocity from the model at the end of a 40 year run. In deriving the analytical solution (12), it is assumed that friction is small except along the east coast of the island. The integrated friction along the east coast of the island must be zero. Figure 6c shows the clockwise integration of along boundary friction around the island starting at the northeastern corner *A*. The northward Kuroshio Current exerts an anticyclonic friction and so the integration between *A* and *B* is negative. The Mindanao Current flows in the opposite direction and exerts a friction that cancels the one induced by the Kuroshio. There are some very small but noticeable contributions from the north and south coast (i.e., from *C* to *D* and from *E* to *A*). Our analyses indicate that the friction along the west coast is small. The integration around the whole island becomes zero.

[40] In our model, the width of the gap is relatively narrow (125 km) and so the WBCs are able to leap over the gaps. In a linear model, whether a WBC can leap through a gap depends on the ratio between the width of the gap and the Munk WBL width [*Sheremet*, 2001]. If the gap is wide, the WBC would not leap through directly but make a detour inside the marginal sea according to Sheremet's analyses. What we would like to emphasize here is that the net LST does not depend on the width of the gap. To demonstrate this point, we conducted another experiment by widening the two connecting straits. The forcing and boundary conditions remain the same. Figure 6b shows the SSH and velocity fields at the end of a 40 year run. The most noticeable change is that the WBCs no longer leap through the gaps directly. They intrude into the marginal sea, turn around along the western boundary and then exit the same straits. The underlying dynamics was discussed by *Sheremet* [2001]. But we would like to emphasize here that the net transport of the throughflow from one strait to the other remains very small (<0.1 Sv) even though the WBCs intrude the marginal sea. So our results remain valid regardless of the width of the gaps. Would the throughflow transport in the model respond to a change in the NEC bifurcation position according to the analytical solution (12)? We ran a series of experiments by moving the position of the NEC meridionally while keeping the two outflow transports, Q_K and Q_M unchanged (both are set to be 20 Sv). For these special cases, the analytical solution (12) becomes:

$$Q_L = \Delta L(Q_M + Q_K)/2L \tag{13}$$

where $L = 875$ km and $Q_M = Q_K = 20$ Sv in the model. Figure 7 shows one example in which the NECBL is moved northward from $y = 0$ to 400 km, i.e., $\Delta L = 400$ km. The analytical solution (13) in this case gives a cyclonic transport (i.e., enters the marginal sea through the northern strait and exits via the southern strait) of $Q_L = 9.14$ Sv. The model produced a throughflow of 7.96 Sv, shown in Figure 7a. The transport in the model is about 13% below the theoretically predicted value of 9.14 Sv. Moving the NEC bifurcation point southward produces an anticyclonic throughflow of 7.77 Sv (Figure 7b), about 15% below the analytical solution (-9.14 Sv). We examined the contributions from the friction along the northern, southern, and western coasts of the island and nonlinearity. They are included in the numerical model but neglected in the analytical solution. Each of them is small according to our diagnoses. But collectively, they affect the model transport by about 10–15% in this experiment.

[41] Figure 7c shows the comparison between the model results (dots) and the theoretical solution (13) (solid line) from 14 different cases. Overall, the model transport is about 10–15% lower than what is expected by the analytical solution (13). The agreement between the model and theory would be nearly perfect if $L = 1000$ km was used in (13) (the solid line in Figure 7c). The zonal width of the island is 100 km in the model. One would attempt to argue that the solution would be nearly perfect if the boundary current length is extended to include the flows along the north and south coast of the island (i.e., extending from $L = 875$ to 975 km in equation (13)). But our diagnoses indicate that friction along the straits is one factor that contributes to the 0–15% difference between the model and theory. Considering the simplicity of the analytical model, this degree of agreement is quite high.

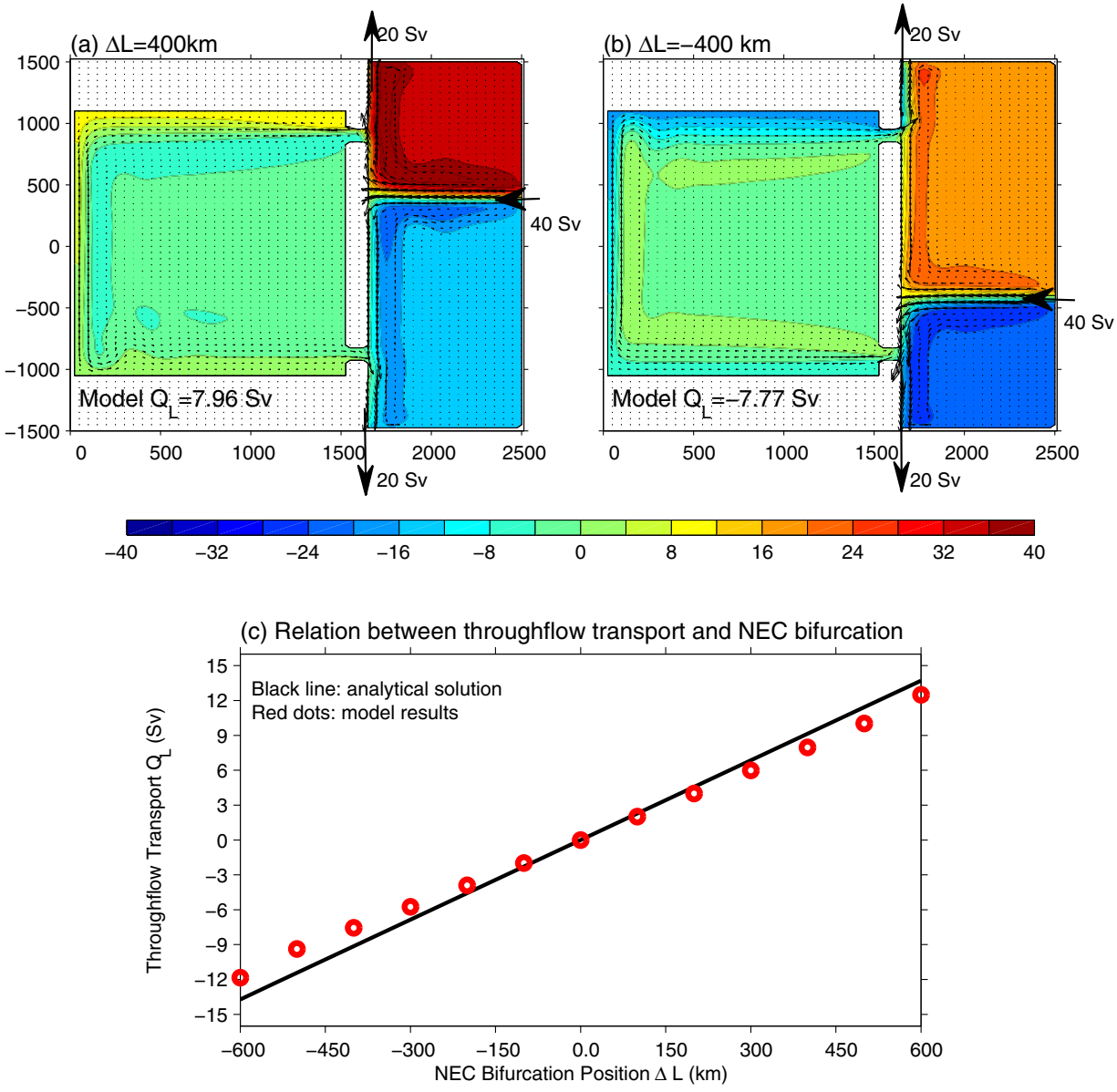

Figure 7. (a) The model result when NEC bifurcation latitude is moved 400 km northward. This induces a cyclonic throughflow (enters the marginal sea through the northern strait) of 7.96 Sv. The model transport is about 13% weaker than the analytical model solution (9.14 Sv); (b) the opposite case when NEC is moved southward; (c) the model-theory comparison of the LST from 14 cases. In all these experiments, the model results are consistent with the analytical model even though the models are about 0–15% weaker than the analytically predicted ones.

4.1.2. Sensitivity to the Partition Between the Mindanao and Kuroshio Current Transports

[42] Next, we will test the model's sensitivity to transports of the Kuroshio and Mindanao Current. For simplicity, we assume that the NECBL is right at the middle position of the island, i.e., $\Delta L = 0$ and thus can simplify the analytical solution (12) to:

$$Q_L = (Q_M - Q_K)/2 \tag{14}$$

[43] The LST, according to (14), would increase when the Mindanao Current strengthens or the Kuroshio Current weakens. To test this, we ran two experiments with different partitions of the two WBC's transports. In the first experiment, the southward WBC, which represents the Mindanao Current, is set to be 26 Sv on the southern boundary, and the northward WBC is specified to be 14 Sv on the northern boundary. The result from this experiment is shown in Figure 8a. The throughflow is cyclonic, i.e., flow enters the marginal sea through the northern strait and exits via the southern strait. The model throughflow transport is 5.16 Sv. It is about 14% weaker than the 6 Sv predicted by the analytical solution (14). If we switch the partition between Kuroshio and Mindanao Currents, the throughflow reverses as shown in Figure 8b. In this second case, the model transport is still about 14% below the

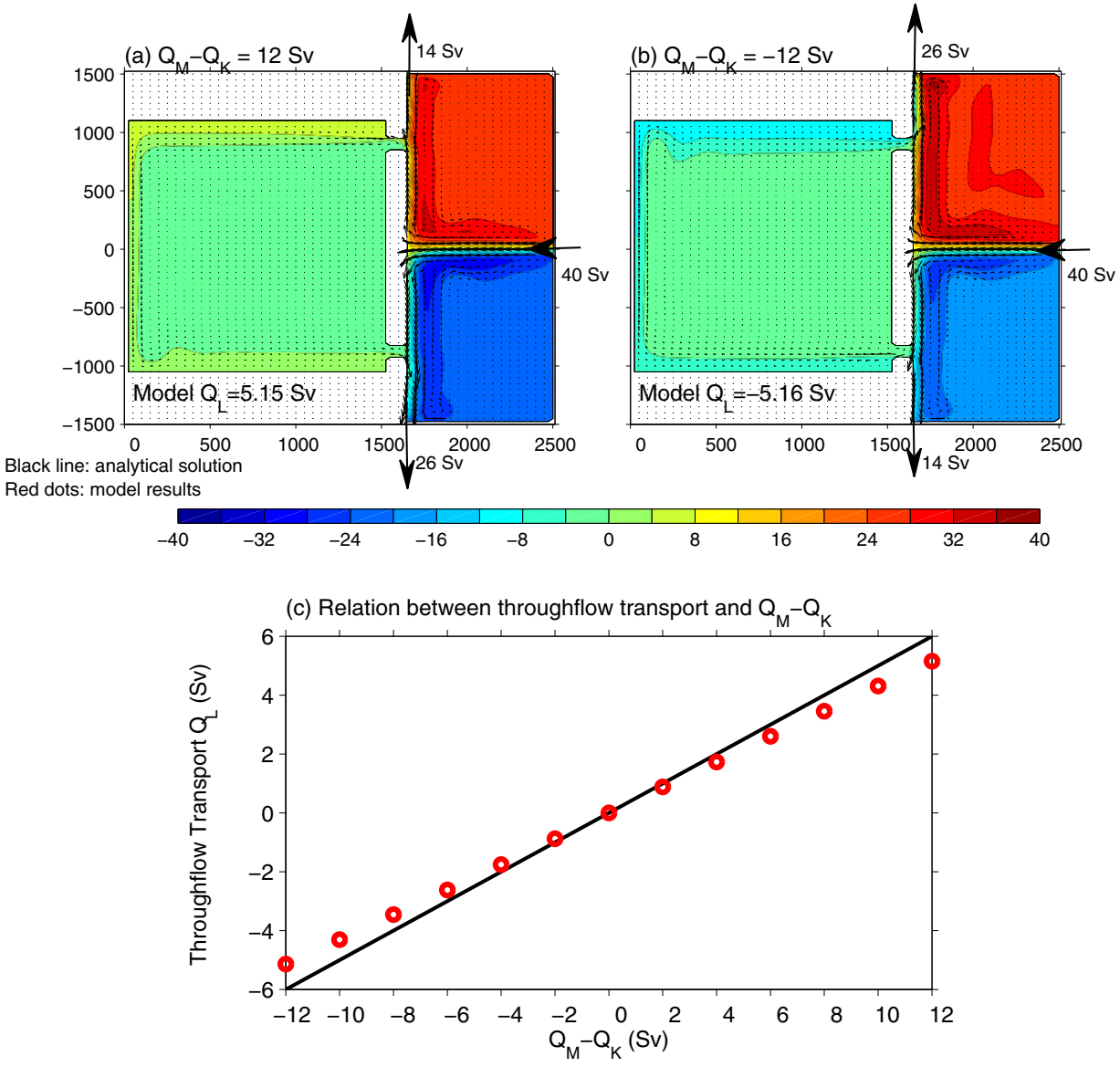

Figure 8. (a) The model SSH (cm) and velocity from an experiment using a stronger MC (26 Sv) and weaker KC (14 Sv). The difference between KC and MC induces a cyclonic throughflow (enters the marginal sea through the northern strait) of 5.16 Sv. The model transport is about 14% weaker than the analytical model solution (6 Sv); (b) for the opposite case with a stronger KC and weaker MC; (c) The model-theory comparison for 14 cases. The model is about 0–15% lower than the theoretically expected transport.

theoretical solution. We conducted several additional experiments and the comparison between the model (red dots) and analytical solution (black line) is shown in the lower panel in Figure 8c. The model transports are 0–15% weaker than the analytical one. The model-theory discrepancy is similar to the previous set of experiments shown in the upper panel in Figure 7c. This cause for the difference is the same as in the previous set of experiments and is due collectively to the neglected friction and nonlinearity in the theoretical model.

4.2. Local Wind-Stress Forcing

[44] The local wind stress has been neglected in the derivation of the analytical solution (12) and in our idealized model experiments. Previous studies indicate that the wind-stress forcing affects the variability of the SCSTF transport [*Metzger and Hurlburt*, 1996]. The local wind-forcing term can be recovered easily. Following the same procedure, equation (12) can be modified to include the local wind-stress forcing term:

$$Q_L = (Q_M - Q_K)/2 + \Delta L(Q_M + Q_K)/2L - \frac{c_0}{\Delta L}\oint_{l=ABCDEA} (\vec{\tau}_{wind}) \cdot d\vec{l} \quad (15)$$

where c_0 is a positive constant and the integration is anticyclonically (clockwise) around the island. A cyclonic wind stress around the island would result in an increase in the LST.

[45] Equation (15) must be consistent with the island rule [*Godfrey*, 1989]. Note that the wind stress along the island's east coast makes no contribution to the throughflow transport in the island rule solution [*Godfrey*, 1989; *Pedlosky et al*., 1997]. But equation (15) seems to suggest that a tangential wind along the east coast would induce a net throughflow transport. How do we reconcile this? The tangential wind stress along a dynamical western boundary (i.e., island's east coast) forces a WBC and is balanced by the friction exerted by this current. For instance, southward wind forces a southward along-boundary current that exerts a northward friction to balance the wind stress. This locally induced WBC component is already included in Q_M and Q_K in (15) because the forcing occurs on the oceanic side of the island. Through the first two terms on the right hand side of (15), the locally induced WBC cancels exactly the local wind stress forcing in (15) and so the tangential wind stress along the east coast makes no contribution to the steady throughflow transport Q_L. Equation (15) is consistent with the island rule solution. But on the seasonal time scale, tangential winds stress along both sides of the island affects the throughflow transport according to our model simulations (both idealized and realistic wind-stress forcing).

5. Discussion and Summary

[46] There is a net transport of the Pacific Ocean water mass into the South China Sea through the Luzon Strait. The LST varies seasonally from a weak to a strong transport from the summer to the fall and winter. Wind-stress forcing over the Pacific Ocean is the main driver for this variability. Previous studies [*Wang et al*., 2006 a, 2006b] have applied the island rule [*Godfrey*, 1989] to the mean and interannual changes in the LST. The island rule is derived from a steady model and is not applicable to the seasonal time scale because the baroclinic adjustment time scale of the subtropical gyre in the North Pacific Ocean is much longer than 1 year. In this study, we have formulated a dynamical model that is more appropriate for the seasonal time scale. It relates the LST to the transports of KC and MC and to the bifurcation latitude of the NEC. It is a steady state model, like the island rule, but the adjustment time scale in this model, when the forcing variables are boundary currents along or near the island, is the time that a Kelvin wave propagates around the island, which is shorter than 1 month for the size of the Philippines.

[47] Our analytical solution shows that the LST into the SCS increases when (1) the NECBL moves northward, (2) the KC transport weakens, or (3) the MC strengthens. Likewise the LST weakens when these conditions reverse. The model is derived from an integral of the momentum equation around the island. The momentum integral results in a balance between the along-shore wind stress and the friction. If the local wind stress is small, the total integral of the friction must vanish. This leads to a balance of the integrated friction induced by the Kuroshio and Mindanao Currents. Using the Munk western boundary layer model, we obtain an analytical solution of the LST that relates to the transports of KC and MC and to the NECBL. The relationship between LST and NECBL-KC-MC in this solution is consistent with previous observation-based studies that the LST is strong in the late fall and early winter when the NECBL moves northward and the KC transport weakens and is weak in the summer when the NECBL shifts southward and the KC strengthens. We have conducted a series of idealized experiments by using a nonlinear and reduced-gravity model. The model results are about 0–15% lower than the theoretically expected values. This is within the range of similar comparisons between numerical models and linear theories in the island rule studies [*Pratt and Pedlosky*, 1998].

[48] We have also used the same reduced-gravity model and a realistic wind stress to simulate the seasonal cycle of the LST. While the phase of the annual evolution of the LST compares favorably with the observation-based estimates (Figure 4a), the magnitude of the modeled LST variations is larger than what was diagnosed from observations by *Yaremchuk and Qu* [2004]. In the model, the NECBL moves northward in the fall, reaching the northernmost position of 13.5N in December, and southward in the summer, to the southernmost latitude of 12.5N in August. The mean position of the NECBL is about 13N, which is roughly the same as what was observed by *Toole et al*. [1988, 1990] but more than 1° south of 14.3N—a position that was estimated by *Yaremchuk and Qu* [2004]. Using the daily output, the maximum seasonal excursion of the NECBL in the model is only about 1.25°, which is much smaller than the 2° variation obtained by *Yaremchuk and Qu* [2004]. The seasonal excursion based on the monthly averaged fields (like in the Yaremchuk and Qu's analyses) is even smaller, 0.75° (Figure 3). *Qiu and Lukas* [1996] also found that the seasonal excursion of the NECBL in their linear reduced-gravity model is only 1°, much smaller than what the meridional movement of the wind-stress curl averaged over the Pacific Ocean would imply. They argued that the Pacific Basin is so wide and that it takes more than a year for baroclinic Rossby waves to travel across the basin. So Rossby waves that originate from the eastern side of the basin may arrive at the coast of the Philippines at the same time as those seasonally opposite waves from the central or western parts of the basins. They hypothesized that the cancellation between these opposite waves results in a very small seasonal excursion in their modeled NECBL. But even a small change in the NECBL could make a major difference according to (13). If we use $2L = 1500$ km (the meridional extent between A and C in Figure 1a), $(Q_K + Q_M) = 60$ Sv, and $\Delta L = 100$ km, equation (13) would imply a change of 4 Sv in the LST merely due to the 100 km shift in the NECBL.

[49] Finally, we will like to note that the NEC is specified as a narrow jet in our idealized experiments. In reality, the NEC is broader meridionally. We have conducted experiments with the NEC to be as broad as 1000 km. The results remain qualitatively the same as the narrow NEC cases.

[50] **Acknowledgments.** This study has been supported by the National Science Foundation Grants (OCE 1028739, 0927017) (JY), and by the Strategic Priority Research Program of the Chinese Academy of Sciences (XDA11010103), the project of Global Change and Air-Sea interaction (GASI-03-01-01-02), the Natural Science Foundation of China (40930844, 41222037), the National Basic Research Program of China (2013CB956202), Ministry of Education's 111 Project (B07036) of China, Yong Science Foundation of Shandong (JQ201111) and Public science and technology research funds projects of ocean (201205018) (XL and DW). We benefit from discussions with Joe Pedlosky, Larry Pratt, and Mike Spall.

References

Centurioni, L. R., P. P. Niiler, and D.-K. Lee (2004), Observations of inflow of Philippine Sea surface water into the South China Sea through the Luzon Strait, *J. Phys. Oceanogr.*, *34*, 113–121.

Farris, A., and M. Wimbush (1996), Wind-induced intrusion into the South China Sea, *J. Oceanogr.*, *52*, 771–784.

Firing, E., B. Qiu, and W. Miao (1999), Time-dependent island rule and its application to time-varying Hawaiian Ridge Current, *J. Phys. Oceanogr.*, *29*, 2671–2688.

Godfrey, J. S. (1989), A Sverdrup model of the depth-integrated flow from the world ocean allowing for island circulations, *Geophys. Astrophys. Fluid Dyn.*, *45*, 89–112.

Jia, Y., and E. P. Chassignet (2011), Seasonal variation of eddy shedding from the Kuroshio intrusion in the Luzon Strait, *J. Oceanogr.*, *67*, 601–611.

Liang, W.-D., Y. J. Yang, T. Y. Tang, and W.-S. Chuang (2008), Kuroshio in the Luzon Strait, *J. Geophys. Res.*, *113*, C08048, doi:10.1029/2007JC004609.

Metzger, E. J., and H. E. Hurlburt (1996), Coupled dynamics of the South China Sea, the Sulu Sea and the Pacific Ocean, *J. Geophys. Res.*, *101*, 12,331–12,352.

Metzger, E. J., and H. E. Hurlburt (2001), The nondeterministic nature of Kuroshio penetration and eddy shedding in the South China Sea, *J. Phys. Oceanogr.*, *31*, 1712–1732.

Nitani, H. (1972), Beginning of the Kuroshio, in *Kuroshio: Its Physical Aspects*, edited by H. Stommel, and K. Yoshida, pp. 129–163, Univ. of Wash. Press, Seattle.

Pedlosky, J., L. Pratt, M. Spall, and K. Helfrich (1997), Circulation around islands and ridges, *J. Mar. Res.*, *55*, 1199–1251.

Pratt, L., and J. Pedlosky (1998), Barotropic circulation around islands with friction, *J. Phys. Oceanogr.*, *298*, 2148–2162.

Qiu, B., and S. Chen (2010), Interannual-to-decadal variability in the bifurcation of the North Equatorial Current off the Philippines, *J. Phys. Oceanogr.*, *40*, 2525–2538.

Qiu, B., and R. Lukas (1996), Seasonal and interannual variability of the North Equatorial Current, the Mindanao Current, and the Kuroshio along the Pacific western boundary, *J. Geophys. Res.*, *101*, 12,315–12,330.

Qu, T., and R. Lukas (2003), The bifurcation of the North Equatorial Current in the Pacific, *J. Phys. Oceanogr.*, *33*, 5–18.

Qu, T., H. Mitsudera, and T. Yamagata (2000), Intrusion of the North Pacific waters into the South China Sea, *J. Geophys. Res.*, *105*, 6415–6424.

Qu, Y., Y. Du, G. Meyers, A. Ishida, and D. Wang (2005), Connecting the tropical Pacific with Indian Ocean through South China Sea, *Geophys. Res. Lett.*, *32*, L24609, doi:10.1029/2005GL024698.

Sheremet, V. (2001), Hysteresis of a western boundary current leaping across a gap, *J. Phys. Oceanogr.*, *31*, 1247–1259.

Tian, J., Q. Yang, X. Liang, L. Xie, D. Hu, F. Wang, and T. Qu (2006), Observation of the Luzon Strait transport, *Geophys. Res. Lett.*, *33*, L19607, doi:10.1029/2006GL026272.

Toole, J. M., E. Zou, and R. C. Millard (1988), On the circulation of the upper waters in the western equatorial Pacific Ocean, *Deep Sea Res., Part A*, *35*, 1451–1482.

Toole, J. M., R. C. Millard, Z. Wang, and S. Pu (1990), Observations of the Pacific North Equatorial Current bifurcation at the Philippine coast, *J. Phys. Oceanogr.*, *20*, 307–318.

Wajsowicz, R. (1993), The circulation of the depth-integrated flow around an island with application to the Indonesian throughflow, *J. Phys. Oceanogr.*, *23*, 1470–1484.

Wang, D., Q. Liu, R. X. Huang, Y. Du, and T. Qu (2006a), Interannual variability of the SouthChina Sea throughflow inferred from wind data and an ocean data assimilation product, *Geophys. Res. Lett.*, *33*, L14605, doi:10.1029/2006GL026316.

Wang, Y., G. Fang, Z. Wei, F. Qiao, and H. Chen (2006b), Interannual variation of the South China Sea circulation and its relation to El Ninõ, as seen from a variable grid global ocean model, *J. Geophys. Res.*, *111*, C11S14, doi:10.1029/2005JC003269.

Wu, C.-R., and Y.-C. Hsin (2012), The forcing mechanism leading to the Kuroshio intrusion into the South China Sea, *J. Geophys. Res.*, *117*, C07015, doi:10.1029/2012JC007968.

Wyrtki, K. (1961), Physical oceanography of the Southeast Asian waters, Naga Rep. 2, 195 pp., Scripps Inst. of Oceanogr., La Jolla, Calif.

Yang, J. (2003), On the importance of resolving the western boundary layer in ocean general circulation models, *Ocean Model.*, *5*, 357–379.

Yang, J., X. Lin, and D. Wu (2013), Wind-driven exchanges between two basins: Some topographic and latitudinal effects, *J. Geophys. Res.*, *118*, 1–15, doi:10.1002/jgrc.20333.

Yaremchuk, M., and T. Qu (2004), Seasonal variability of the large scale currents near the coast of Philippines, *J. Phys. Oceanogr.*, *34*, 844–855.

Yaremchuk, M., J. McCreary, Z. Yu, R. Furue (2009), The South China Sea throughflow retrieved from climatological data, *J. Phys. Oceanogr.*, *39*, 753–767, doi: 10.1175/2008JPO3955.1.

Yu, Z., S. Shen, J. P. McCreary, M. Yaremchuk, and R. Furue (2007), South China Sea throughflow as evidenced by satellite images and numerical experiments, *Geophys. Res. Lett.*, *34*, L01601, doi:10.1029/2006GL028103.